OPEN ACCESS

Short report

Premorbid brain structure influences risk of amyotrophic lateral sclerosis

Alexander G Thompson, Bernd Taschler, Stephen M Smith, Martin R Turner

► Additional supplemental material is published online only. To view, please visit the journal online (http://dx.doi.org/10.1136/jnnp-2023-332322).

Nuffield Department of Clinical Neurosciences, University of Oxford, Oxford, UK

Correspondence to
Dr Alexander G Thompson, Nuffield Department of Clinical Neurosciences, University of Oxford, Oxford, UK; alexander.thompson@ndcn.ox.ac.uk
Dr Martin R Turner; martin.turner@ndcn.ox.ac.uk

Received 27 July 2023
Accepted 25 September 2023

To cite: Thompson AG, Taschler B, Smith SM, *et al*. *J Neurol Neurosurg Psychiatry* Epub ahead of print: [*please include* Day Month Year]. doi:10.1136/jnnp-2023-332322

ABSTRACT

Background Amyotrophic lateral sclerosis (ALS) is a disease of the motor network associated with brain structure and functional connectivity alterations that are implicated in disease progression. Whether such changes have a causal role in ALS, fitting with a postulated influence of premorbid cerebral architecture on the phenotypes associated with neurodegenerative disorders is not known.

Methods This study considered causal effects and shared genetic risk of 2240 structural and functional MRI brain scan imaging-derived phenotypes (IDPs) on ALS using two sample Mendelian randomisation, with putative associations further examined with extensive sensitivity analysis. Shared genetic predisposition between IDPs and ALS was explored using genetic correlation analysis.

Results Increased white matter volume in the cerebral hemispheres was causally associated with ALS. Weaker causal associations were observed for brain stem grey matter volume, parieto-occipital white matter surface and volume of the left thalamic ventral anterior nucleus. Genetic correlation was observed between ALS and intracellular volume fraction and isotropic free water volume fraction within the posterior limb of the internal capsule.

Conclusions This study provides evidence that premorbid brain structure, in particular white matter volume, contributes to the risk of ALS.

INTRODUCTION

The clinical manifestations of amyotrophic lateral sclerosis (ALS) occur due to neuronal loss within the corticomotoneuronal system and its wider connections in a clinicopathological spectrum with frontotemporal dementia (FTD).[1] Regional neuronal loss influenced by premorbid nervous system characteristics is a broad hypothesis for selective vulnerability across the neurodegenerative disorders.[2–6] The incidence of ALS in relation to age supports a multistep model of pathogenesis.[7]

Marked changes in cerebral connectivity are demonstrable with MRI during the symptomatic phase of ALS.[8] Loss of white matter integrity is consistently observed within the corpus callosum and cerebral corticospinal tracts, but also more extensively,[9 10] alongside reduced grey matter volume within the primary motor cortex,[10] frontal lobes and subcortical structures,[11 12] particularly the thalamus.[13] Structural alterations have been associated with connectivity changes based on resting-state blood oxygen level-dependent (BOLD) functional MRI.[14–17]

Altered brain structure and function are detectable in asymptomatic carriers of highly penetrant ALS-causing genetic variants, many years prior to expected symptom onset.[18–21] These changes could represent early events in pathogenesis, imply shared genetic determinants of ALS and brain connectivity, reflect a developmental phenotype, represent a causal hit in a multistep model,[22] or indicate more fundamental differences in brain development or ageing associated with specific genetic variants.[23] Changes observed in such cohorts are of uncertain relevance to the majority of people with ALS, in whom the disease is not associated with monogenetic variants, instead resulting from a convergence of more complex genetic influences, ageing, environmental factors and stochastic events.[24]

Mendelian randomisation (MR) employs genetic variants randomly allocated at meiosis as instrumental variables (IVs) to infer causal effects of one trait on another (figure 1, reviewed in Sanderson *et al*[25]). This approach has been used to explore relationships between imaging features and psychiatric disease.[26 27] This study applied two-sample MR using genome wide association studies (GWAS) of imaging-derived phenotypes (IDPs), representing structural (T1 and diffusion-based) and functional (resting-state BOLD) cerebral measures as 'exposures' and ALS as the 'outcome of interest' to identify causal effects of IDPs, along with studying shared genetic risk of IDPs and ALS using linkage disequilibrium score regression genetic correlation (LDSC).

MATERIALS AND METHODS

A statistical analysis plan was uploaded to the Open Science Framework prior to undertaking the analysis (https://osf.io/xv6nd/). Summary statistics from GWAS of IDPs for 33 224 European ancestry UK Biobank participants aged 46–82 were used to identify exposure IVs.[28] A manually curated set of 335 motor system IDPs and a full set of 2240 IDPs were considered as exposures (online supplemental tables 1 and 2). The outcome GWAS comprised 20 806 European ancestry ALS patients (a mixture of sporadic and familial ALS) and 59 804 control participants.[29] A second outcome GWAS of 27 205 European ancestry ALS patients and 110 881 control participants, which includes raw data from the first GWAS but employs a different statistical approach was used for further validation of IDPs.[30] Reported results refer to the first ALS GWAS. Findings in the second GWAS are reported in online supplemental

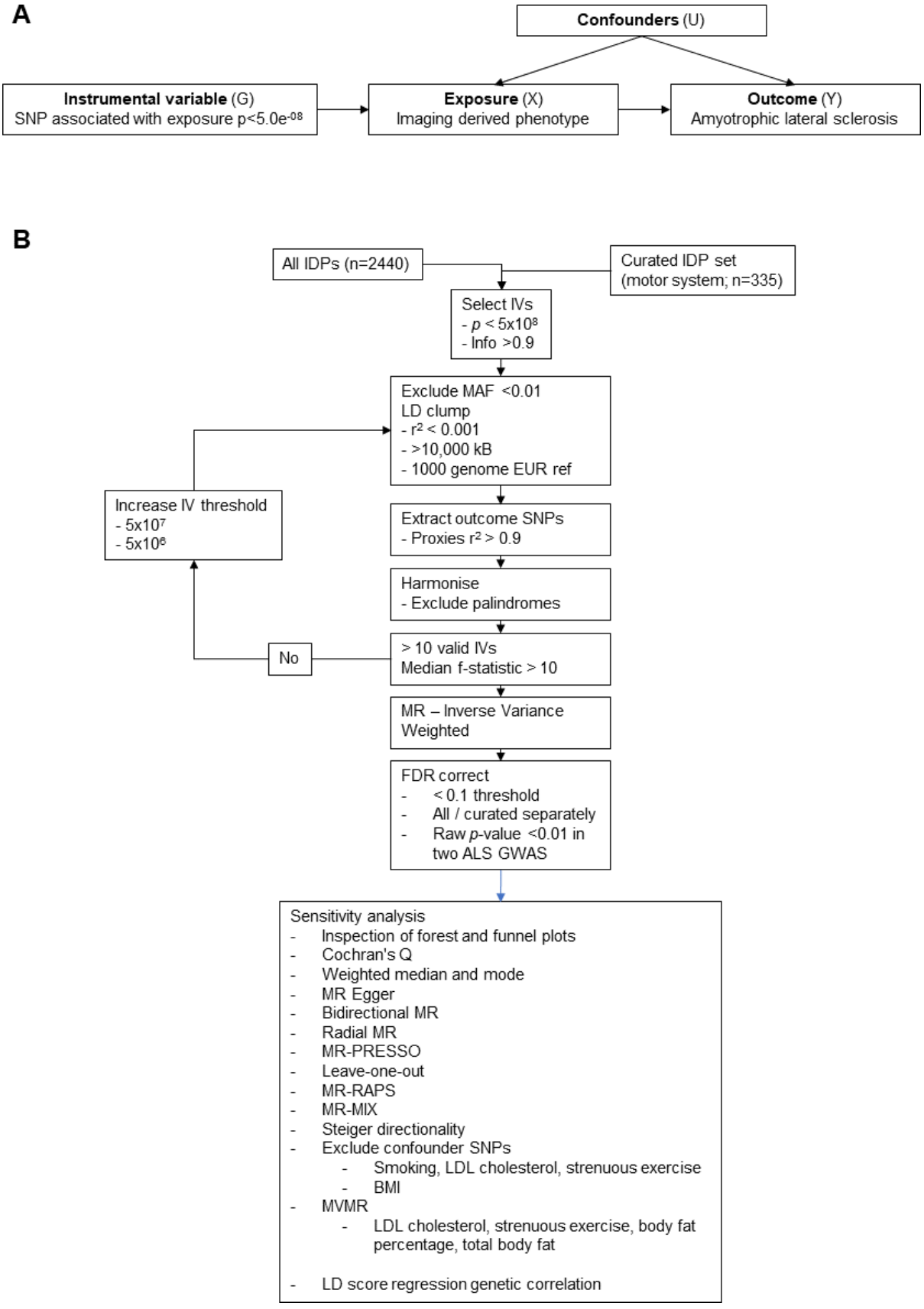

Figure 1 (A) Mendelian randomisation uses randomly assorted genetic alleles (G) as instrumental variables to probe causal influences of an exposure (X) on an outcome of interest (Y), independent of confounding effects on the exposure and outcome. (B) Workflow of the Mendelian randomisation approach used. ALS, amyotrophic lateral sclerosis; EUR, European ancestry; FDR, false discovery rate; IDP, imaging derived phenotype; IV, instrumental variable; LD, linkage disequilibrium; MAF, minor allele frequency; MR-Mix, Mendelian randomisation using mixture models; MR-PRESSO, MR Pleiotropy RESidual Sum and Outlier; MR-RAPS, MR using a Robust Adjusted Profile Score; MVMR, multivariable MR; SNP, single-nucleotide polymorphism.

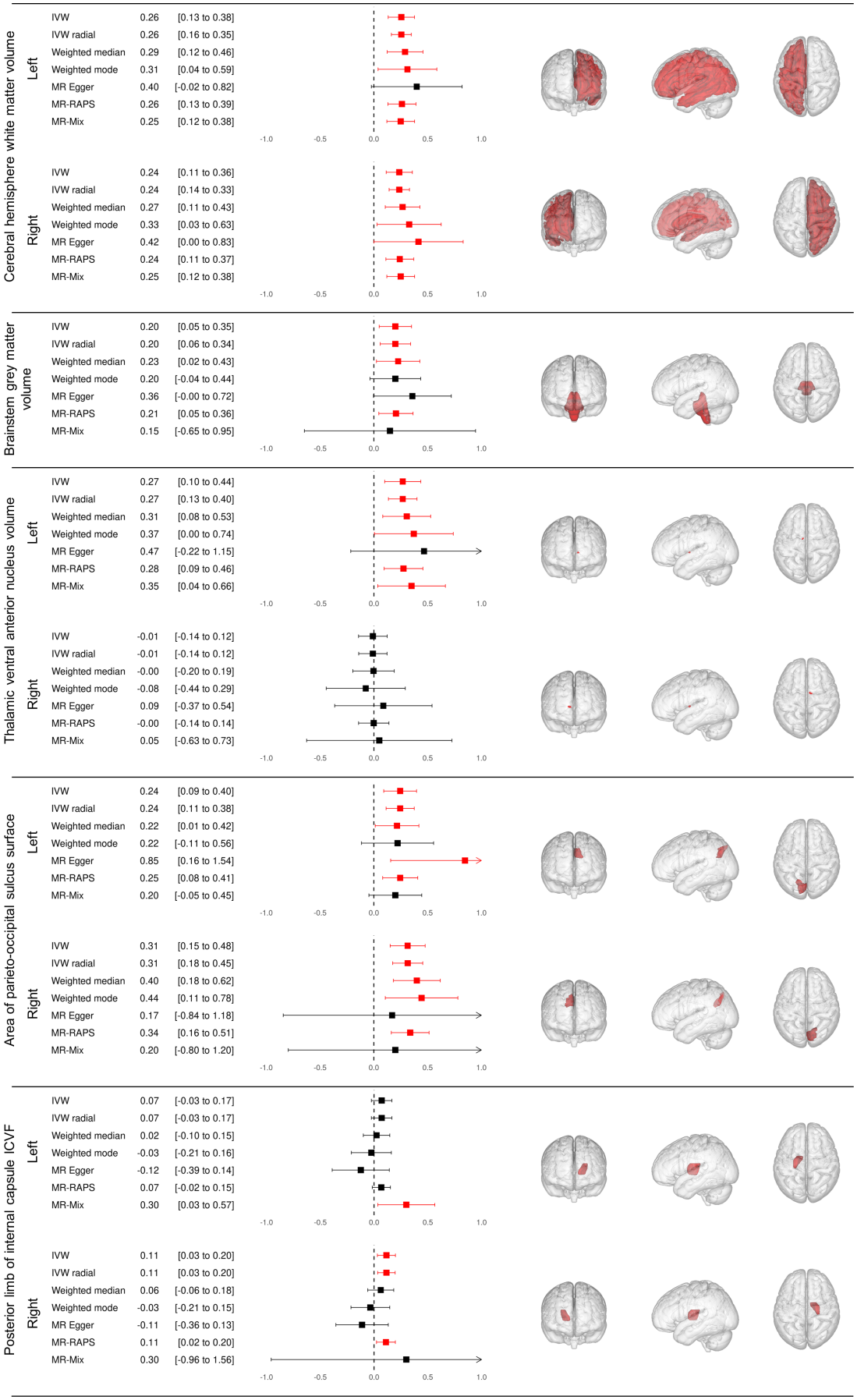

Figure 2 Sensitivity analysis of significant IDPs. Red error bars indicate analyses with p<0.05. ICVF, intracellular volume fraction; IVW, inverse variance-weighted; MR-Mix, Mendelian randomisation using mixture models; MR-RAPS, MR using a Robust Adjusted Profile Score.

tables. Precomputed LD scores from 1000 Genomes European reference were used, restricted to single-nucleotide polymorphisms (SNPs) with minor allele frequency >0.01 and high-quality imputation (INFO>0.9) in the UK Biobank imputed dataset, excluding multiallelic SNPs.

MR analysis was performed using TwoSampleMR and gwasVCF packages in R.[31] SNPs with genome wide significance for the relevant IDP ($p<5\times10^{-8}$) were clumped by LD $r^2<0.001$, window size 10 000 kB. Proxy SNPs with $r^2>0.9$ were substituted for IVs absent from the outcome dataset. IVs were harmonised between exposure and outcome. Palindromic SNPs were excluded. If <10 SNPs remained with median f-statistic>10, the genome wide significance threshold was relaxed (to $<5\times10^{-7}$ then $<5\times10^{-6}$) and the procedure repeated. If fewer than 10 SNPs remained with median f-statistic>10, the IDP was omitted.

Initial MR was performed using inverse variance weighted (IVW) analysis. FDR correction was applied to the curated set of 335 IDPs then the full set of 2240 IDPs, with FDR-adjusted p<0.1 considered statistically significant to proceed to sensitivity analysis. Analysis was repeated using a second outcome GWAS.[30] IDPs with raw p<0.01 in both outcome GWAS were additionally taken forward for sensitivity analysis in variance from the prespecified analysis plan.

Sensitivity analyses accounting for instrument heterogeneity, horizontal pleiotropy, weak instrument bias, outliers and reverse causality were performed, using leave-one-out analysis, Cochran's Q test, weighted median and mode, MR Egger, bidirectional MR, Steiger directionality, MR-RAPS, MR-PRESSO, MR-MIX, repeating IVW analysis excluding genome-wide SNPs associated with the potential confounders smoking, low density lipoprotein cholesterol, strenuous exercise and body mass index.[26 32] To explore the possibility of causal effects being mediated by other exposures associated with ALS risk using MR, we also undertook multivariable MR including body fat percentage, total body fat mass, strenuous exercise or other activity and LDL cholesterol as covariates.

Genetic correlation analysis was performed using LDSC.[33] Analysis was initially performed with the intercept constrained and using default settings. To increase statistical power, the intercept was constrained to zero, selecting additional IDPs with FDR-adjusted p<0.1 in either GWAS and p<0.05 in both GWAS with the intercept unconstrained.

RESULTS

IVW MR identified a single IDP with FDR-adjusted p<0.1—hemispheric cerebral white matter volume by subcortical volume segmentation (effect estimates for IVW MR; left hemisphere β=0.26, 95% CI 0.13 to 0.38, p<0.001, FDR-adjusted p=0.096; right hemisphere β=0.24, 95% CI 0.11 to 0.36, p<0.001, FDR-adjusted p=0.111). Findings were consistent in the second ALS GWAS and all sensitivity analyses indicated robust causal associations (figure 2). Full IVW MR results are provided in online supplemental table 3.

Five IDPs (nine including contralateral IDPs) had unadjusted p<0.01 in both ALS GWAS and a consistent direction of causal association. Of these, brain stem grey matter volume (β=0.20, 95% CI 0.05 to 0.35, p=0.009, FDR-adjusted p=0.723), area of the surface of the parieto-occipital sulcus (left hemisphere β=0.24, 95% CI 0.09 to 0.40, p<0.001, FDR-adjusted p=0.386; right hemisphere β=0.31, 95% CI 0.15 to 0.48, p<0.001, FDR-adjusted p=0.111) and volume of the left ventral anterior nucleus of the thalamus (β=0.27, 95% CI 0.10 to 0.44, p=0.002, FDR-adjusted p=0.386; figure 2; online supplemental table 4) were robust to sensitivity analysis.

In genetic correlation analysis, 36 IDPs had FDR-adjusted p<0.1 in at least 1 ALS GWAS with the intercept constrained to zero, of which 4 had unadjusted p<0.05 in both ALS GWAS when analysed with the intercept unconstrained: mean intracellular volume fraction within the corticospinal tract in both hemispheres (a measure of neurite density; unconstrained genetic correlation r_g=0.311, p=0.007, FDR-adjusted p=0.156 right; r_g=0.266, p=0.024, FDR-adjusted p=0.223 left) and mean intensity of the thalamus in both hemispheres generated by subcortical volume segmentation (unconstrained r_g=0.198, p=0.013, FDR-adjusted p=0.112 right; r_g=0.186, p=0.030, FDR-adjusted p=0.112 left; table 1).

Three additional bilateral IDPs had uncorrected p<0.01 and concordant direction of association in both ALS GWAS with the intercept unconstrained (table 1 and online supplemental table 3): a further white matter microstructural measure, mean isotropic free water volume fraction in the posterior limb of the internal capsule (unconstrained r_g=0.380, p=0.008, FDR-adjusted p=0.112 right; r_g=0.316, p=0.024, FDR-adjusted p=0.333 left), volume of grey matter in the planum polare (unconstrained r_g=0.230, p=0.014, FDR-adjusted p=0.710 right; r_g=0.256, p=0.006, FDR-adjusted p=0.710 left) and grey-white contrast in the precentral gyrus of the left hemisphere calculated as a percentage of the mean grey-white matter intensity from Desikan-Killiany parcellation (unconstrained r_g=−0.243, p=0.006, FDR-adjusted p=0.710 right; r_g=−0.248, p=0.005, FDR-adjusted p=0.710 left; full results of genetic correlation analysis online supplemental table 3).

DISCUSSION

Systematically applying genomic analysis methods to explore the relationship between imaging-measured brain variation and risk of ALS identified brain structural features with evidence of causal effects on ALS and features that share genetic predisposition with ALS. The strongest associations were of a causal effect of hemispheric white matter volume on ALS risk and genetic correlation between corticospinal tract microstructure and ALS. With the exception of white matter volume in the left hemisphere, IDP associations were not significant at the prespecified 10% FDR threshold, though they were consistent in magnitude and direction with nominally significant unadjusted p values in contralateral structures and using two ALS outcome GWAS. The MR findings were also robust to extensive sensitivity analysis.

White matter volume, predominantly comprising myelin, increases through childhood and adolescence before slowly decreasing after the fourth decade, showing tract-specific variation.[34]

There is evidence for activity-dependent white matter plasticity occurring most markedly during childhood but persisting into adulthood for a range of cognitive and motor tasks.[35–37] Higher white matter volumes have been associated with higher total body fat, though multivariable MR indicates that the causal relationship between ALS and white matter volume is not mediated through total body fat mass.[38] White matter volume decreases with ageing and correlates with cognitive performance, though factors governing the rate of white matter loss are not known, and volume loss is not associated with white matter hyperintensities.[39]

Alterations in white matter microstructure, specifically reduced neurite density in the corticospinal tracts, have been demonstrated at presymptomatic timepoints in carriers of a

Table 1 Genetic correlations between IDP and ALS

Description		Left		Right	
		r_g	P value	r_g	P value
Mean intra-cellular volume fraction in corticospinal tract on fractional anisotrophy skeleton	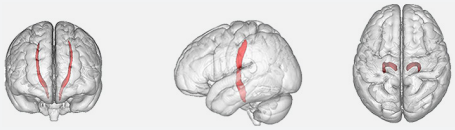	0.266	0.024	0.311	0.007
Mean intensity of thalamus-proper generated by subcortical volume segmentation		0.186	0.030	0.198	0.013
Mean isotropic or free water volume fraction in posterior limb of internal capsule on fractional anisotrophy skeleton		0.316	0.024	0.380	0.008
Volume of grey matter in planum polare		0.256	0.006	0.230	0.014
Grey-white contrast in precentral calculated as a percentage of mean grey-white matter intensity from Desikan-Killiany parcellation		−0.248	0.005	−0.243	0.006

ALS, amyotrophic lateral sclerosis; IDP, imaging-derived phenotype; r_g, genetic correlation.

C9orf72 hexanucleotide repeat expansion (HRE), the most common monogenic cause of ALS and FTD.[40] Presymptomatic alterations in brain volume have been observed in carriers of ALS and FTD-causing genetic variants in early adulthood, with carriers of FTD-causing *MAPT* and *GRN* variants having higher total intracranial volume compared with noncarriers, but lower total intracranial volume observed in *C9orf72* HRE carriers.[41] Although these findings are divergent, they suggest potential neurodevelopmental mechanisms in FTD and ALS.

The relationship between hemispheric white matter volume and risk of ALS might, therefore, be a consequence of differences in brain development during adolescence or childhood, activity-dependent morphological changes, alterations in motor system ageing, or the effect of systemic metabolic variables on brain morphology. Overall this study primarily provides converging evidence for brain white matter structure as an upstream element of the vulnerability to ALS, supporting a broad concept that brain structural variation influences risk of neurodegeneration.

Contributors All authors contributed to study design. AGT undertook the analysis, prepared the figures and manuscript. All authors reviewed and edited the manuscript.

Funding AGT holds a Clinician Scientist Fellowship from the Medical Research Council (MR/T006927/1) and Lady Edith Wolfson Fellowship from the Motor Neuron Disease Association (Thompson/Jan20/952-795). Computation used the Oxford Biomedical Research Computing (BMRC) facility, a joint development between the Wellcome Centre for Human Genetics and the Big Data Institute supported by Health Data Research UK and the NIHR Oxford Biomedical Research Centre. This research was funded in whole, or in part, by the UKRI MR/T006927/1.

Disclaimer The views expressed are those of the authors and not necessarily those of the NHS, the NIHR or the Department of Health.

Competing interests None declared.

Patient consent for publication Not applicable.

Provenance and peer review Not commissioned; externally peer reviewed.

ORCID iDs
Alexander G Thompson http://orcid.org/0000-0003-1063-3277
Martin R Turner http://orcid.org/0000-0003-0267-3180

REFERENCES

1 Hardiman O, Al-Chalabi A, Chio A, *et al*. Amyotrophic lateral sclerosis. *Nat Rev Dis Primers* 2017;3.
2 Bak TH, Chandran S. What wires together dies together: verbs, actions and neurodegeneration in motor neuron disease. *Cortex* 2012;48:936–44.
3 Eisen A, Turner MR. Does variation in neurodegenerative disease susceptibility and phenotype reflect cerebral differences at the network level *Amyotroph Lateral Scler Frontotemporal Degener* 2013;14:487–93.
4 Eisen A, Turner MR, Lemon R. Tools and talk: an evolutionary perspective on the functional deficits associated with amyotrophic lateral sclerosis. *Muscle Nerve* 2014;49:469–77.
5 Mattsson N, Schott JM, Hardy J, *et al*. Selective vulnerability in neurodegeneration: insights from clinical variants of alzheimer's disease. *J Neurol Neurosurg Psychiatry* 2016;87:1000–4.
6 Seeley WW, Crawford RK, Zhou J, *et al*. Neurodegenerative diseases target large-scale human brain networks. *Neuron* 2009;62:42–52.
7 Al-Chalabi A, Calvo A, Chio A, *et al*. Analysis of amyotrophic lateral sclerosis as a multistep process: a population-based modelling study. *Lancet Neurol* 2014;13:1108–13.

8 Agosta F, Spinelli EG, Filippi M. Neuroimaging in amyotrophic lateral sclerosis: current and emerging uses. *Expert Rev Neurother* 2018;18:395–406.
9 Filippini N, Douaud G, Mackay CE, *et al*. Corpus callosum involvement is a consistent feature of amyotrophic lateral sclerosis. *Neurology* 2010;75:1645–52.
10 Bede P, Bokde A, Elamin M, *et al*. Grey matter correlates of clinical variables in amyotrophic lateral sclerosis (ALS): a neuroimaging study of ALS motor phenotype heterogeneity and cortical focality. *J Neurol Neurosurg Psychiatry* 2013;84:766–73.
11 Agosta F, Gorno-Tempini ML, Pagani E, *et al*. Longitudinal assessment of grey matter contraction in amyotrophic lateral sclerosis: a tensor based morphometry study. *Amyotroph Lateral Scler* 2009;10:168–74.
12 Bede P, Elamin M, Byrne S, *et al*. Basal ganglia involvement in amyotrophic lateral sclerosis. *Neurology* 2013;81:2107–15.
13 Tu S, Menke RAL, Talbot K, *et al*. Regional thalamic MRI as a marker of widespread cortical pathology and progressive frontotemporal involvement in amyotrophic lateral sclerosis. *J Neurol Neurosurg Psychiatry* 2018;89:1250–8.
14 Douaud G, Filippini N, Knight S, *et al*. Integration of structural and functional magnetic resonance imaging in amyotrophic lateral sclerosis. *Brain* 2011;134(Pt 12):3470–9.
15 Proudfoot M, Bede P, Turner MR. Imaging cerebral activity in amyotrophic lateral sclerosis. *Front Neurol* 2018;9:1148.
16 Agosta F, Canu E, Valsasina P, *et al*. Divergent brain network connectivity in amyotrophic lateral sclerosis. *Neurobiol Aging* 2013;34:419–27.
17 Verstraete E, van den Heuvel MP, Veldink JH, *et al*. Motor network degeneration in amyotrophic lateral sclerosis: a structural and functional connectivity study. *PLoS One* 2010;5:e13664.
18 Menke RAL, Proudfoot M, Wuu J, *et al*. Increased functional connectivity common to symptomatic amyotrophic lateral sclerosis and those at genetic risk. *J Neurol Neurosurg Psychiatry* 2016;87:580–8.
19 Bertrand A, Wen J, Rinaldi D, *et al*. Early cognitive, structural, and microstructural changes in presymptomatic *c9orf72* carriers younger than 40 years . *JAMA Neurol* 2018;75:236.
20 Querin G, Bede P, El Mendili MM, *et al*. Presymptomatic spinal cord pathology in C9Orf72 mutation carriers: a longitudinal neuroimaging study. *Ann Neurol* 2019;86:158–67.
21 Carew JD, Nair G, Andersen PM, *et al*. Presymptomatic spinal cord neurometabolic findings in Sod1-positive people at risk for familial ALS. *Neurology* 2011;77:1370–5.
22 Chiò A, Mazzini L, D'Alfonso S, *et al*. The Multistep hypothesis of ALS revisited the role of genetic mutations. *Neurology* 2018;91:e635–42.
23 van Veenhuijzen K, Westeneng H-J, Tan HHG, *et al*. Longitudinal effects of asymptomatic C9Orf72 carriership on brain morphology. *Ann Neurol* 2023;93:668–80.
24 Al-Chalabi A, Hardiman O. The epidemiology of ALS: a conspiracy of genes, environment and time. *Nat Rev Neurol* 2013;9:617–28.
25 Sanderson E, Glymour MM, Holmes MV, *et al*. Mendelian randomization. *Nat Rev Methods Primers* 2022;2:6.
26 Taschler B, Smith SM, Nichols TE. Causal inference on neuroimaging data with Mendelian randomisation. *Neuroimage* 2022;258.
27 Guo J, Yu K, Dong S-S, *et al*. Mendelian randomization analyses support causal relationships between brain imaging-derived phenotypes and risk of psychiatric disorders. *Nat Neurosci* 2022;25:1519–27.
28 Smith SM, Douaud G, Chen W, *et al*. An expanded set of genome-wide association studies of brain imaging phenotypes in UK biobank. *Nat Neurosci* 2021;24:737–45.
29 Nicolas A, Kenna KP, Renton AE, *et al*. Genome-wide analyses identify Kif5A as a novel ALS gene. *Neuron* 2018;97:S0896-6273(18)30148-X:1268–1283..
30 van Rheenen W, van der Spek RAA, Bakker MK, *et al*. Common and rare variant association analyses in amyotrophic lateral sclerosis identify 15 risk Loci with distinct genetic architectures and neuron-specific biology. *Nat Genet* 2021;53:1636–48.
31 Hemani G, Zheng J, Elsworth B, *et al*. The MR-base platform supports systematic causal inference across the human phenome. *Elife* 2018;7:e34408.
32 Neale Lab UK Biobank GWAS, Available: http://www.nealelab.is/uk-biobank/
33 Bulik-Sullivan BK, Loh P-R, Finucane HK, *et al*. LD score regression distinguishes confounding from polygenicity in genome-wide Association studies. *Nat Genet* 2015;47:291–5.
34 Lebel C, Gee M, Camicioli R, *et al*. Diffusion tensor imaging of white matter tract evolution over the lifespan. *Neuroimage* 2012;60:340–52.
35 Bengtsson SL, Nagy Z, Skare S, *et al*. Extensive piano practicing has regionally specific effects on white matter development. *Nat Neurosci* 2005;8:1148–50.
36 Scholz J, Klein MC, Behrens TEJ, *et al*. Training induces changes in white-matter architecture. *Nat Neurosci* 2009;12:1370–1.
37 Dziemian S, Appenzeller S, von Bastian CC, *et al*. Working memory training effects on white matter integrity in young and older adults. *Front Hum Neurosci* 2021;15.
38 Dekkers IA, Jansen PR, Lamb HJ. Obesity, brain volume, and white matter microstructure at MRI: a cross-sectional UK Biobank study. *Radiology* 2019;292:270.
39 Christiansen P, Larsson HB, Thomsen C, *et al*. Age dependent white matter lesions and brain volume changes in healthy volunteers. *Acta Radiol* 1994;35:117–22.
40 Wen J, Zhang H, Alexander DC, *et al*. Neurite density is reduced in the presymptomatic phase of C9Orf72 disease. *J Neurol Neurosurg Psychiatry* 2019;90:387–94.
41 Finger E, Malik R, Bocchetta M, *et al*. Neurodevelopmental effects of genetic frontotemporal dementia in young adult mutation carriers. *Brain* 2023;146:2120–31.